99. Nucleic-Acid Analogs with Restricted Conformational Flexibility in the Sugar-Phosphate Backbone ('Bicyclo-DNA')

Part 6[1])

Probing the Influence of Torsion Angle γ on DNA-Duplex Stability: Synthesis and Properties of Oligodeoxynucleotides Containing [(3'*S*,5'*S*)-2'-Deoxy-3',5'-ethano-β-D-ribofuranosyl]adenine and -thymine ('5'-Epi-bicyclodeoxynucleosides')[2])

by **J. Christopher Litten**[3]) and **Christian Leumann***

Institut für Organische Chemie, Universität Bern, Freiestrasse 3, CH-3012 Bern

(10.IV.96)

The synthesis of the thymine- and adenine-containing 5'-epi-bicyclodeoxynucleosides **7** and **8** as well as of the corresponding building blocks **13** and **14** for oligonucleotide synthesis according to the phosphoramidite methodology is described. A conformational analysis of **7** and **8** by ^{1}H-NMR spectroscopy, refined by molecular modeling, shows the preferred conformation of the furanose unit in these nucleosides to be of the 1'-*exo*/2'-*endo* type. The 5'-OH group on the carbocyclic ring prefers to be axially oriented, thus placing torsion angle γ in the unusual $-$*syn*-clinal ($-sc$) range. These epi-bicyclodeoxynucleosides were successfully incorporated into DNA decamers. From UV/melting curves of such decamers with DNA and RNA complements, a duplex destabilization of -2 to $-9°$ per residue was observed. An oligonucleotide built completely from 5'-epi-bicyclothymidine shows no detectable affinity to its DNA or RNA complement anymore. CD Spectra of duplexes containing 5'-epi-bicyclodeoxynucleotide units are very similar to the natural reference systems, indicating no major structural changes. A molecular-dynamics simulation of a heptamer duplex containing one 5'-epibicyclothymidine residue in the center reveals a conformational change of its carbocyclic unit placing torsion angle γ in the (for the free mononucleoside unfavorable) $-$*anti*-clinal ($-ac$) conformation in the duplex. The role of torsion angle γ on DNA duplex stability is discussed.

1. Introduction. – The role of structure and flexibility of the sugar-phosphate backbone in DNA and RNA on order, base-association mode, selectivity, and energy in complex formation can experimentally be addressed by design, synthesis, and analysis of DNA analogs displaying well defined structural modifications. Knowledge gained from such studies not only promotes the current understanding of the supramolecular chemistry of DNA and RNA but may also be of direct relevance in antisense and antigene research [3–5].

Within this area, we recently developed the DNA analog 'bicyclo-DNA', exhibiting reduced conformational flexibility, imparted by an additional carbocyclic ring between

[1]) Part 5: [1].

[2]) Preliminary communication: [2].

[3]) Present address: *Ciba-Geigy Ltd.*, R&D Plant Protection, CH-4002 Basel.

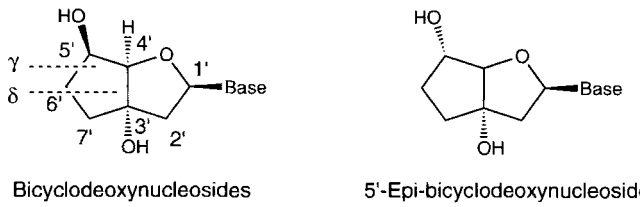

Fig. 1. *Numbering scheme and composition of bicyclo- and 5'-epi-bicyclodeoxynucleosides*

the centers C(3') and C(5') of the underlying bicyclodeoxynucleosides (*Fig. 1*) [6][4]). After having first addressed the question on how reduced backbone flexibility influences the energy of complex formation [7] [8], we recently turned our attention to the structural consequences of the sugar modification on the base-pairing properties. Analysis of duplex formation of homopurine and homopyrimidine sequences revealed a structural preorganization of the bicyclo-DNA backbone preferring the *Hoogsteen*- and reversed-*Hoogsteen*- over the *Watson-Crick*-association mode [9]. This change in the mode of strand recognition can directly be related to the consequences of a shift of the backbone torsion angle γ by *ca.* +100°, relative to that found in DNA duplexes of the A- and B-type (*Fig. 2*).

Besides this, the nature of the carbocyclic ring in the bicyclodeoxynucleoside skeleton permits a further extension of the study of the influence of torsion angle γ on DNA duplex structure and stability. Inversion of configuration at the center C(5') (to give the 5'-epi-bicyclodeoxynucleosides, *Figs. 1* and *2*) constrains the C(5')–O(5') bond, and thus torsion angle γ, to the *–anti*-clinal (*–ac*) or *–syn*-clinal (*–sc*) conformational space. While natural deoxynucleosides can in principle adopt this geometry, it is rarely observed on the level of mononucleosides and not found in DNA complexes with a regular mononucleotide repeating backbone unit [10].

Here we wish to report on the synthesis, the preferred conformation in solution, and molecular modeling studies of the 5'-epi-bicyclodeoxynucleosides containing the bases adenine and thymine, as well as on the synthesis and analysis of the base-pairing properties of oligonucleotides thereof.

2. Synthesis of '5'-Epi-bicyclodeoxynucleosides'. – Starting from the known bicyclodeoxynucleosides β-D-**1** and β-D-**2**, we initially attempted to invert the configuration at the center C(5') under *Mitsunobu* reaction conditions [11]. However, despite a number of trials and screening a variety of carboxylic acids as nucleophiles, this method failed in our hands in these specific cases. We, therefore, chose to effect inversion by the classical approach. Selective mesylation of the secondary OH group in the anomeric mixtures of bicyclothymidine (α/β-D-**1**) and N^6-benzoylbicyclodeoxyadenosine (α/β-D-**2**; prepared as described in [4]), followed by chromatography[5]) yielded the corresponding β-configu-

[4]) For a description of the nomenclature and numbering scheme used to describe bicyclo-DNA, see [6] (Footnote 3).

[5]) We reported earlier that a bulky silyl group, such as the (*tert*-butyl)dimethylsilyl group, at O–C(5') was required for a successful chromatographic separation of the anomers [6]. In the case of the anomeric mixtures **3** and **4**, described here, the mesyl function at O–C(5') already led to sufficient chromatographic differentiation so that the mixtures were cleanly resolved by MPLC in both cases.

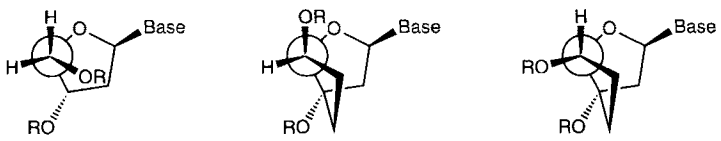

Fig. 2. Newman *projection along the C(4′)–C(5′) bond* (torsion angle γ) *in natural, bicyclo-, and 5′-epi-bicyclodeoxynucleosides*

rated mesylates **3** and **4** (*Scheme*). The assignment of the anomeric form in **3** and **4** was possible by comparison of the coupling pattern of the anomeric protons in their ^{1}H-NMR spectra with that of the parent bicyclonucleosides. Direct inversion reactions on **3** and **4** using CsOAc in DMSO produced up to 40% of elimination products besides the desired epi-bicyclodeoxynucleosides, as identified by ^{1}H-NMR. We observed, however, that this side reaction could be suppressed by conversion of the tertiary OH group in an ester function prior to inversion. Therefore, **3** and **4** were acetylated to give **5** and **6**. Under the reaction conditions chosen (the presence of the catalyst 4-(dimethylamino)pyridine was required for acylation of the tertiary OH), concomittant *N*-acylation of the benzamido function at the base moiety of **4** occurred. Inversion at C(5′) in **5** and **6** was then effected by displacement of the mesylate group by acetate (CsOAc) in DMSO at 70–90° to give the diacetates **7** and **8** exclusively. Interestingly the N^6-acetyl function in **6** was cleanly lost during the reaction. Selective saponification of the diacetates **7** and **8** finally produced the epi-bicyclonucleosides **9** and **10** in 86 and 85% yields, respectively. Subsequent treatment of **9** and **10** with an excess of $[(MeO)_2Tr]CF_3SO_3$ [8] yielded the corresponding trityl derivatives **11** and **12**. Performance of this reaction at room temperature was satisfactory with **9** (64%), but low (< 30%) with **10**. In the latter case, the yield was substantially increased (78%) by carrying out the reaction at 40°. The tritylated 5′-epi-bicyclodeoxynucleosides were then elaborated to the corresponding phosphoramidite building blocks by reaction with chloro(2-cyanoethoxy)(diisopropylamino)phosphine in dry THF. The reaction proceeded in the same manner as in the case of the bicyclodeoxynucleosides and produced **13** and **14** as diastereoisomer mixtures (*ca.* 1:1 ratio as determined by ^{1}H- and ^{31}P-NMR) in yields of 78 and 65%, respectively. These phosphoramidites were subsequently used in the automated solid-phase oligonucleotide synthesis.

3. Conformational Analysis of the 5′-Epi-bicyclodeoxynucleosides. – 3.1. *General.* A conformational analysis of the bicyclodeoxynucleosides based on X-ray and ^{1}H-NMR analysis has previously been reported [6]. The results from this analysis showed that the furanose ring uniformly adopts the 1′-*exo*/2′-*endo* conformation with the C(5′) substituent adopting the pseudoequatorial position, thus placing the torsion angle γ in the +*ap* range (*Fig. 3, a*). In the series of the epi-bicyclodeoxynucleosides described here, we have performed a similar conformational analysis based on ^{1}H-NMR spectroscopy combined with molecular modeling.

Scheme

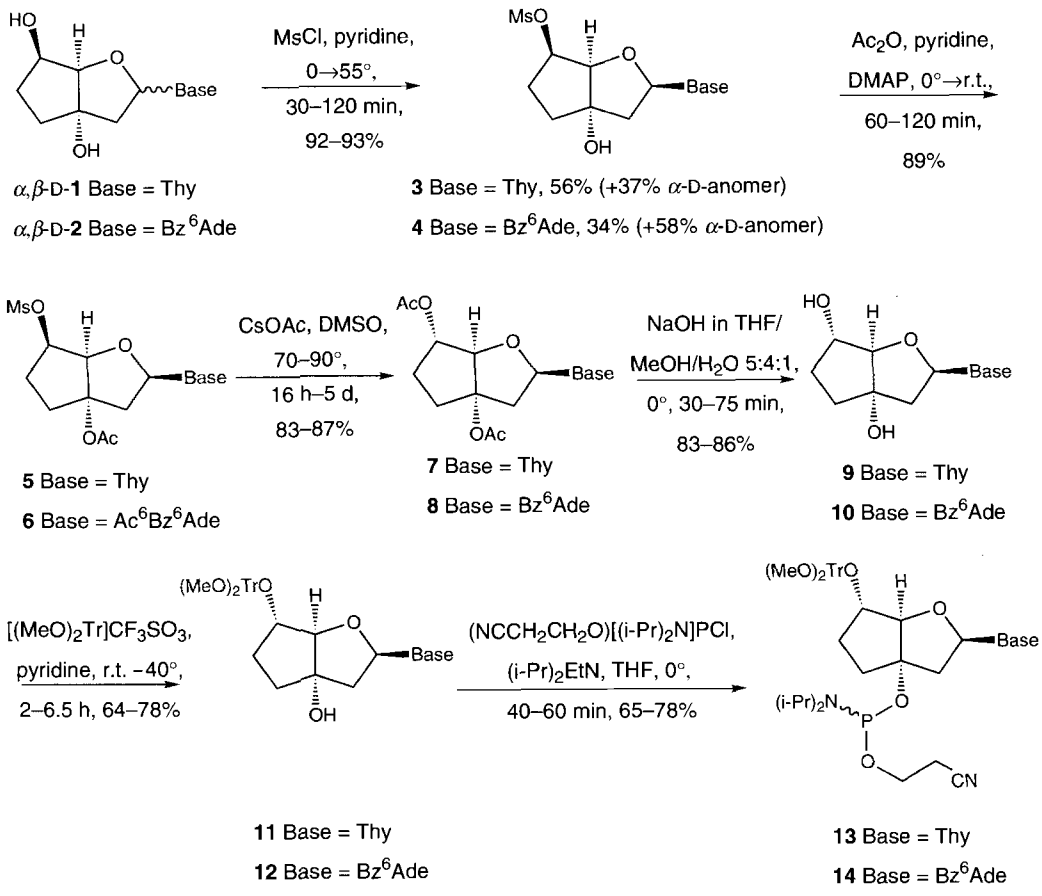

3.2. *Conformation of the 5′-Epi-bicyclodeoxynucleosides in Solution.* Due to the H-coupling barrier at C(3′), it is not possible to directly calculate the dihedral angles of interest for the carbohydrate scaffold in the 5′-epi-bicyclodeoxynucleosides from their ^{1}H-NMR data. However, a computer model can be constructed with the experimentally determined dihedral angles γ and ν_1[6]), calculated from the corresponding ^{1}H-NMR coupling data, forced onto the bicyclic system. In this way, the remaining dihedral angles can be measured from the energy-minimized structure[7]). The torsion angles ν_1 and γ were ob-

[6]) Notations and abbreviations used for the structural and conformational description of 5′-epi-bicyclodeoxynucleosides are in accord with the IUPAC rules for natural nucleosides and nucleotides [12].

[7]) The bicyclic structures **7** and **8** were built and subjected to a full matrix *Newton-Raphson* minimization (*Amber** forcefield) to a RMS gradient < 0.01 as implemented by BatchMin, available with Macro-Model (version 4.5) [13], with the experimentally determined torsion angles ($^3J(1',2'\alpha)$, $^3J(1',2'\beta)$, $^3J(4',5')$) being imposed on the structure with a force constant of 9000 kJ·mol^{-1}. After minimization in this way, the resulting dihedral angles were measured directly from the structure.

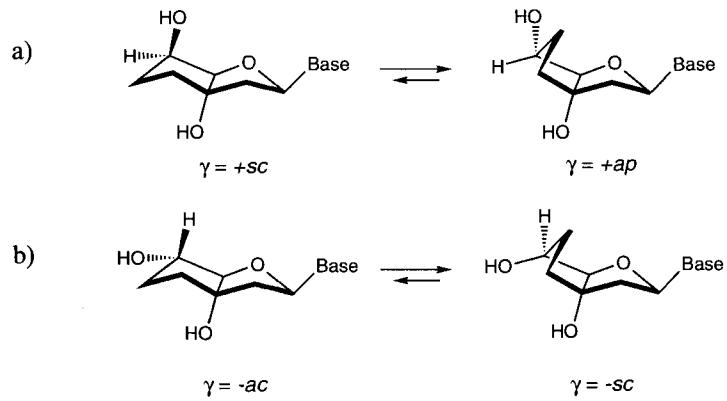

Fig. 3. *Preferred ring conformations of* a) *bicyclo- and* b) *5'-epi-bicyclodeoxynucleosides*

tained by determination of the dihedral angles between the protons H–C(1')/H_α–C(2'), H–C(1')/H_β–C(2'), and H–C(4')/H–C(5') using the *Karplus* relationship optimized for nucleosides and nucleotides [14]. The values for all relevant torsion angles determined as well as the pseudorotation phase angle *P* for **7** and **8** are presented in *Table 1*. Inspection of these data lead to the firm conclusion that the furanose units in **7** and **8** occur preferentially in the 1'-*exo* range, while torsion angles γ lie in the –*sc* range, thus orienting the secondary OH groups in the pseudoaxial position.

The preferred conformation about the nucleosidic bond χ was determined in the case of **7** *via* ^{1}H-NMR NOE difference spectroscopy (in $CDCl_3$). On irradiation at the resonance of the base proton H–C(6) (7.10 ppm), positive NOE's were observed at 1.98 ppm (H_β–C(2')), 6.12 ppm (H–C(1')), and 5.01 ppm (H–C(5')). A weak negative NOE was observed at H_α–C(2') (2.85 ppm) that is most likely due to an indirect NOE through H_β–C(2'). From a comparison of the relative intensities of NOE's at H–C(1') and H_β–C(2'), it is possible to estimate the population of *syn-* and *anti-*forms using the

Table 1. *Selected Chemical Shifts* [ppm], *Coupling Constants* J [Hz] *of Protons, and Furanose Ring Torsion Angles of the 5'-Epi-bicyclodeoxynucleosides* **7** *and* **8**

	δ [ppm]					$^3J(1',2'\alpha)$[a])	$^3J(1',2'\beta)$[a])	$^2J(2'\alpha,2'\beta)$[a])	$^3J(4',5')$[a])
	H–C(1')	H_α–C(2')	H_β–C(2')	H–C(4')	H–C(5')				
7	6.12	2.85	1.98	4.34	5.01	5.3 (40°)	9.5 (157°)	14.7	< 1.0 (*ca.* ±90°)
8	6.41	3.02	2.46	4.54	5.07	6.3 (45°)	8.7 (150°)	14.9	< 1.0 (*ca.* ±90°)

Dihedral angles [°] for the furanose units in **7** and **8** obtained as described in the text

	ν_0	ν_1[b])	ν_2	ν_3	ν_4	γ[a])	δ	P[b])	pucker
7	–40.6	35.0	–16.9	–6.3	29.7	–86.4	116.5	115.0	C(1')-*exo*
8	–38.7	32.9	–15.2	–7.5	29.7	–85.7	116.0	113.0	C(1')-*exo*

[a]) In parentheses, torsion angles calculated from the corresponding coupling constants.
[b]) Pseudorotation phase angle.

relationship developed by *Seela* and coworkers [15]. The NOE experiment gave a ratio of *ca.* 0.55 and, therefore, indicates a slight advantage of the *anti*-orientation over the *syn*-orientation by 60–65%.

3.3. *Molecular Modeling of the 5′-Epi-bicyclodeoxynucleoside* **7**. Unconstrained molecular modeling was carried out in addition to the ^{1}H-NMR solution studies. We modeled the thymine-containing nucleoside **7** with the molecular-modeling package MacroModel (version 4.5) [13]. Conformational searching[8]) of **7** lead, after energy minimization, to only two conformers **7A** and **7B** (*Fig. 4*, top and bottom, respectively) corresponding to two local energy minima. The conformer **7A** shows the furanose part in a 1′-*exo* conformation with the values for the torsion angles γ and δ being −91.6 and 122.0°, respectively, while conformer **7B** has a 2′-*endo*-type sugar pucker with torsion

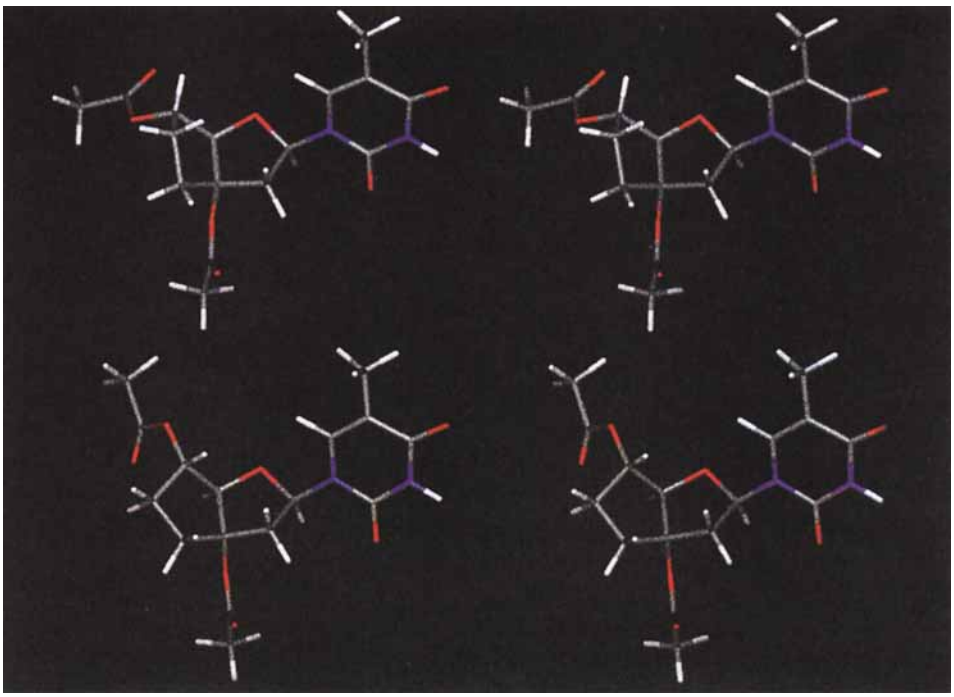

Fig. 4. *Stereoscopic views of energy-minimized conformers of 5′-epi-bicyclothymidine* **7**: *conformers* **7A** (top) *and* **7B** (bottom)

[8]) An initially built structure of **7** was minimized and subjected to a 100-ps dynamics simulation at 600 K, with the glycosidic bond χ constrained to the *anti*-range (−90°), structure sampling was carried out at 1-ps intervals, using the BatchMin implementation of the Amber* forcefield and the GB/SA [16] continuous water solvation treatment. This lead to a set of 100 structures, which were minimized using the full-matrix *Newton-Raphson* method, to a RMS gradient < 0.01 (maximum 500 iterations). A structural comparison of all the minimized conformers was undertaken, in which all heavy atoms were compared; those structures in which there was a RMS difference of > 0.25 Å were considered to belong to a unique conformational class. In this way two distinct groups of conformers were found.

angles γ and δ of -167.4 and 140.1°, respectively. This clearly indicates that the main structural differences between **7A** and **7B** lie within the conformation of the carbocyclic rings. The conformer **7A** shows the 5′-OH group in the pseudoaxial orientation and, therefore, the torsion angle γ in the $-sc$ range, whereas in conformation **7B** the 5′-OH group is found in the pseudoequatorial arrangement and places γ into the $-ac$ range. The two structures differ by 2.28 kcal·mol^{-1}, with the conformer **7A** having the OH group axially oriented being lower in energy.

Conformer **7A** compares very well with the experimentally determined conformation of **7** and clearly underlines the preference for the axial over equatorial orientation of the secondary OH group in the epi-bicyclodeoxynucleosides (*Fig. 3, b*). *Therefore, the nature of the bicyclic scaffold and not the substituent at C(5′) determines the conformational properties of the carbocyclic ring unit.*

4. Synthesis of Oligomers. – The syntheses of the oligomers **15–21** (*Table 2*) were carried out on a DNA synthesizer on the 1.3-μmol scale. In the synthesis cycle, only the parameters for detritylation and coupling time were changed to 60 s and 14 min, respectively, relative to the assembly of natural DNA oligomers. For synthetic convenience, commercially available deoxycytidine-loaded controlled pore glass (CPG) was used as the starting unit for **18**. The concentration of the phosphoramidite and phosphoramidite/1*H*-tetrazole ratio remained unchanged. Coupling yields for **13** and **14**, as monitored *via* trityl assay, were on the average of 85%, and were less efficient than in the corresponding bicyclodeoxynucleotide series. Chain assembly was completed by removal of the last trityl group followed by detachment from the solid support and deprotection under standard conditions (conc. NH_3, 55°, 10–16 h)[9]).

The crude oligomers were purified by HPLC on an anion-exchange and/or reversed-phase stationary phase to homogeneity. The integrity of the oligomers was confirmed by matrix-assisted laser-desorption-ionization time-of-flight mass spectrometry (MALDI-

Table 2. *Composition of 5′-Epi-bicyclodeoxynucleoside-Containing Oligomers* **15–21** *and the 'Mismatch' Sequence* **22**[a])

	Sequence
15	5′-d(T-T-T-T-T-T-T-T-T-T)-3′
16	5′-d(T-T-T-T-**T**-T-T-T-T-T)-3′
17	5′-d(T-T-T-**T**-T-T-T-T-T-T)-3′
18	5′-d(**T-T-T-T-T-T-T-T-T-T**-C)-3′
19	5′-d(A-A-A-A-A-A-A-A-A-A)-3′
20	5′-d(A-A-A-A-A-A-A-A-A-A)-3′
21	5′-d(A-A-A-A-A-A-A-A-A-A)-3′
22	5′-d(T-T-T-T-T-C-T-T-T-T)-3′

[a]) **T** = 5′-Epi-bicyclothymidine; **A** = 5′-epi-bicyclodeoxyadenosine; A, T, C = natural 2′-deoxynucleosides.

[9]) The synthesis of the natural oligodeoxynucleotides, used as references or as duplexation complements, were performed according to the standard procedures using commercially available phosphoramidite building blocks. Purification of all oligomers was effected by HPLC (see *Exper. Part*).

TOF-MS) using a matrix optimized for nucleic-acid analysis [17] (see *Exper. Part*). The mass spectra showed the molecular monoanion as the main peak, together with signals at higher m/z, which could be assigned to sodium and/or potassium complexes of the corresponding molecular ions[10]). The oligomers were chemically stable and showed no signs of degradation under the conditions used for the subsequent analysis by UV/melting curves and CD spectroscopy (HPLC control).

5. Pairing Behavior of 5′-Epi-bicyclodeoxynucleotide-Containing Oligomers. – Complementary duplex formation of the oligomers **15**–**18** with $d(A)_{10}$, the bicyclo-DNA complement $bcd(A)_{10}$, and poly(rA), and the oligomers **19**–**21** with $d(T)_{10}$, $bcd(T)_{10}$, and poly(rU) as well as of combinations leading to complementary 5′-epi-bicyclodeoxynucleotide base pairs (*i.e.*, **15**·**19**, **16**·**20**, and **17**·**21**) were followed by UV/melting curves (1M NaCl, pH 7.0) at 260 nm. A representative selection can be found in *Fig. 5*. The melting temperatures (T_m), relative hyperchromicites, and ΔT_m per modification (ΔT_m/mod.), relative to the natural reference oligomer sequences, obtained from these experiments are presented in *Table 3*. All melting curves showed reversible, cooperative behavior on repeated heating and cooling cycles. At duplex concentrations of 3.9–4.3

Table 3. T_m [°] *Values, Hyperchromicites* (% at 260 nm; in parentheses) *and* ΔT_m/*Modification Values* [°] (in italics) *of 5′-Epi-bicyclodeoxynucleotide-Containing Duplexes as Determined from UV/Melting Curves.* Conc. 3.9–4.5 μM; buffer: 1M NaCl, 10 mM NaH_2PO_4, pH 7.0.

	$d(A_{10})$	poly(rA)	$bcd(A_{10})$	$d(T_{10})$	poly(rU)	$bcd(T_{10})$	**19**	**20**	**21**
15	26.3 (23%) *−4.9*[a])	30.7 (16%) *−4.9*[b])	37.1 (12%) *−6.3*[c])				24.5 (23%) *−6.7*[a])		
16	20.2 (10%) *−6.5*[a])	22.5 (12%) *−6.6*[b])	30.4 (5%) *−6.5*[c])					13.7 (6%) *−8.8*[a])	
17	25.8 (14%) *−2.7*[a])	25.5 (19%) *−5.1*[b])	31.8 (12%) *−5.8*[c])						21.7 (12%) *−4.8*[a])
18	[d])	[d])	[d])						
19				29.6 (11%) *−1.6*[a])	54.9 (25%) *−2.7*[e])	19.5 (14%) *−7.5*[f])			
20				25.8 (18%) *−2.7*[a])	53.0 (47%) *−2.3*[e])	18.0 (9%) *−4.5*[f])			
21				28.8 (25%) *−1.2*[a])	54.6 (36%) *−1.5*[e])	18.4 (17%) *−4.3*[f])			
$d(A_{10})$				31.2 (30%)	57.6 (40%)	27.0 (27%)			
$d(T_{10})$	31.2 (30%)	35.6 (37%)	43.4 (34%)						
22	8.9 (16%) *−22.3*[a])	19.5 (15%) *−16.1*[b])	20.5 (12%) *−22.9*[c])						

[a]) ΔT_m/mod. with respect to $d(T_{10})\cdot d(A_{10})$. [b]) ΔT_m/mod. with respect to $d(T_{10})\cdot$poly(rA). [c]) ΔT_m/mod. with respect to $d(T_{10})\cdot bcd(A_{10})$. [d]) No melting transition observed. [e]) ΔT_m/mod. with respect to $d(A_{10})\cdot$poly(rU). [f]) ΔT_m/mod. with respect to $d(A_{10})\cdot bcd(T_{10})$.

[10]) The difference between the experimentally determined mass (m/z) and the calculated molecular mass of the monoanions is within the tolerance of the instrument (1‰). The only exception is the oligomer **19** (1.4‰) which exceeds that limit. The reason for this is unknown, but the difference in mass is too small to indicate an alternative structure to that which we propose.

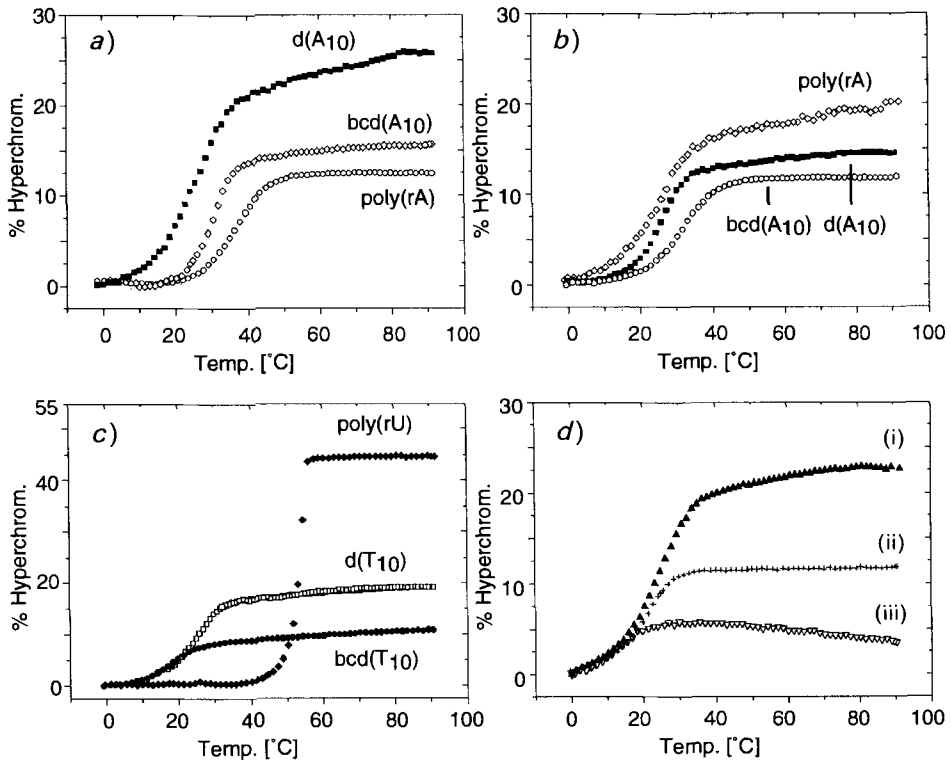

Fig. 5. *UV/Melting curves of 1:1 mixtures of* a) **15**, b) **17**, *and* c) **20**, *with the complements indicated and of* d) **15**/**19** (i), **17**/**21** (ii), **16**/**20** (iii) *in 1* M *NaCl, 10 m*M NaH_2PO_4 (pH 7, c = 3.9–4.3 μmol)

μmol and 1:1 strand ratios, triple-helix formation of the *Hoogsteen* type could be excluded in all systems due to the nonexistence of melting transitions at 284 nm [18][11]).

Replacement of one thymidine or deoxyadenosine residue by the corresponding 5′-epi-bicyclodeoxynucleotide in the center of a decamer sequence (**15** and **19**) causes a significant reduction in the pairing efficiency to its DNA, RNA, or bicyclo-DNA complement. It is not surprising, therefore, to observe that, when two modified 5′-epi-bicyclodeoxynucleotide derivatives (**16**, **17**, **20**, and **21**) are placed in a decamer sequence, the pairing efficiency is further reduced. Additionally, a decamer block of 5′-epi-bicyclodeoxythymidine units (sequence **18**) was not observed to pair with its complement under the conditions used.

It is important to note that for all matched duplexes with the 5′-epi-bicyclodeoxynucleotide-containing sequences **15**–**17** and **19**–**21**, the ΔT_m/mod. (−1.6 to −6.6°) are

[11]) In the case of the duplex **15**·d(A_{10}), a second transition at lower temperature, visible at both wavelength 260 and 284 nm, was observed in the UV/melting curves at duplex concentrations > 7 μM. This may indicate concentration-dependent *Hoogsteen*-type base pairing occurring in this system.

significantly less than that of the deliberate mismatched duplex **22**·d(A_{10}), with a cytosine opposite an adenine rest (ΔT_m/mod. −23°, *Table 3*). This is a clear indication that the duplexes containing 5′-epi-bicyclodeoxynucleotides are matched structures but are significantly destabilized.

In the cases in which the two 5′-epi-bicyclodeoxynucleotide residues are arranged in a contiguous fashion (**16** and **20**), the ΔT_m/mod. was found to be approximately twice the value of that in which the oligomers had a single modification (**15** and **19**). Where the two 5′-epi-bicyclonucleotides are spaced by a natural 2′-deoxynucleotide (**17** and **21**), the ΔT_m/mod. is found to be less than that of a single modification, and about half of that found in the contiguous derivatives. The same behavior was observed previously in alternating sequences of natural 2′-deoxynucleotides and bicyclodeoxynucleotides [8]. The rationale for this is that the strain built up by the structurally rigid bicyclodeoxysugar is in part relieved by the interrupts of the more flexible natural 2′-deoxynucleotides.

A stronger duplex destabilization (ΔT_m/mod. −4.3 to −7.5°) is observed when the oligomers **15**–**17** and **19**–**21** were paired with complementary bicyclo-DNA (bcd(A_{10}) or bcd(T_{10})). Again, this destabilization cannot be considered as a mismatched base pair. It rather expresses unfavorable local geometric arrangements of the bases brought about by the two conformationally restricted types of nucleosides.

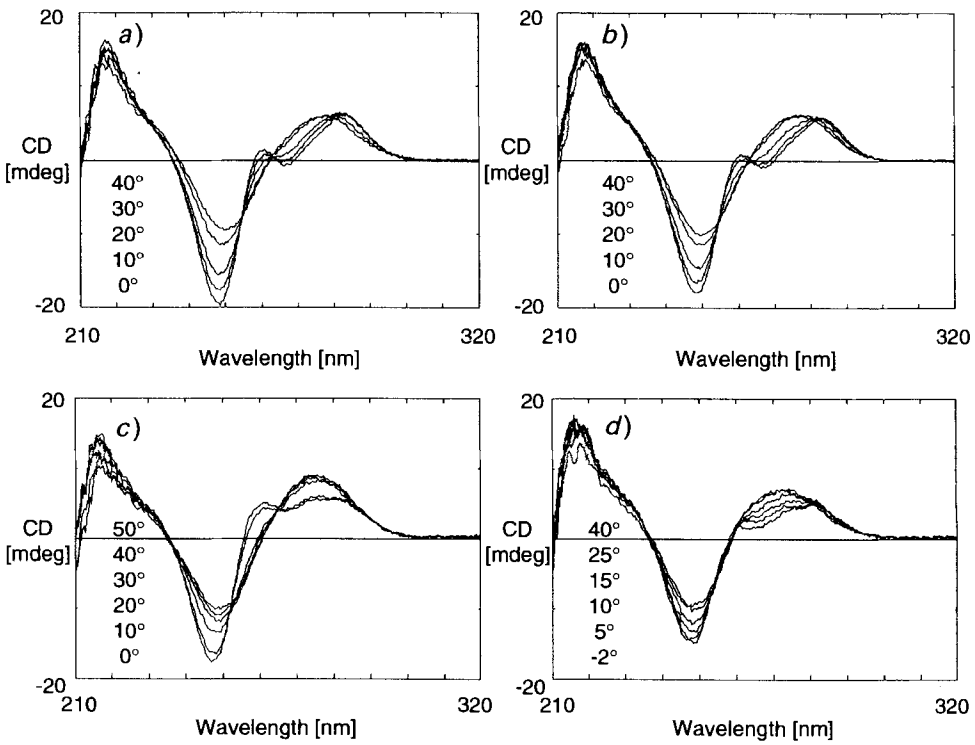

Fig. 6. *CD Spectra of* a) **15**·*d*(A_{10}), b) **17**·*d*(A_{10}), c) **21**·*bcd*(T_{10}), d) **16**·**20** *in 1* M *NaCl, 10 m*M NaH_2PO_2 (pH 7, *c* = 3.9–4.3 μmol)

The 5′-epi-bicyclodeoxynucleotides facing each other in the duplex, as in **15·19**, **16·20**, and **17·21** are the most destabilizing combinations investigated in this study. Relative to the reference duplex $d(T_{10})\cdot d(A_{10})$, the ΔT_m/mod. data can be as high as −8.8°. Again, the destabilization is reduced when a natural 2′-deoxynucleotide is placed between the two modified nucleotides (**17·21**).

The CD spectra (representative selection in *Fig. 6*) of the complementary duplexes **15**, **16**, and **17** with $d(A_{10})$, and **19**, **20**, and **21** with $d(T_{10})$ are very similar to that of $d(T_{10})\cdot d(A_{10})$. This indicates that with neither one nor two modifications there is any significant change in binding mode or conformation with respect to the natural reference system. The duplexes are, therefore, aligned in an antiparallel fashion exhibiting *Watson-Crick* base pairing.

6. 3′-Exonuclease Resistance of the 5′-Epi-bicyclodeoxynucleotides. – The stability of the undecamer **18** was examined against the 3′-exonuclease, snake-venom phosphodiesterase, by UV spectroscopy. A rapid (but relatively small) initial increase in absorption at 260 nm was observed, most likely caused by the cleavage of the 3′-terminal 2′-deoxycytidine residue. This was followed by a much slower increase of absorption, indicating the cleavage of the remaining phosphodiester groups. The undecamer **18** was fully degraded after 285 min (*cf.* 3 min for $d(T_{10})$ and 205 min for $bcd(T_{10})$). The 5′-epi-bicyclodeoxynucleotides, therefore, show considerable enhancement of resistance to the 3′-exonucleases over the natural system. They show only a small increase in resistance over the bicyclo-DNA decamer, thus indicating that snake-venom phosphodiesterase does not discriminate between bicyclo- or 5′-epi-bicyclodeoxynucleotides as substrates. Obviously the relative configuration at the center C(5′) is of less importance for the activity of this enzyme.

7. Molecular Modeling. – To gain insight into the possible structure of duplexes containing 5′-epi-bicyclodeoxynucleotides, we modeled the heptamer duplex [d(T-T-T-Y-T-T-T)]·[d(A-A-A-A-A-A-A)], where Y corresponds to a 5′-epi-bicyclothymidine residue. This duplex closely resembles that of **15**·$d(A_{10})$. The 5′-epi-bicyclosugar unit with an axially oriented 5′-OH group ($\gamma = -sc$) was accomodated in the center of this B-DNA duplex, and a dynamics simulation on a 200-ps trajectory (298 K) was performed (for details see *Exper. Part*). A stereoview of the average duplex structure of the last 10 ps is given in *Fig. 7*, a detailed stereoview of the 5′-epi-bicyclothymidine residue at the beginning (top) and at the end (bottom) of the dynamics run is given in *Fig. 8*.

The main structural change observed during the dynamics simulation has its origin in a conformational change of the carbocyclic part of the epi-bicyclonucleotide unit, placing the corresponding torsion angle γ from the (favored) $-sc$ in the (unfavored) $-ap$ conformational range. This shift is accompanied by a concomittant change of torsion angle α from the $+sc$ to the $+ap$ (*trans*) range and is associated with an extension of the intrastrand base distance, thus resembling the backbone structure in DNA intercalator complexes (see *e.g.* [19]).

The conformational change can be rationalized as follows: from construction of the initial model it becomes clear that the best fit to accomodate a nucleotide unit with torsion angle γ in the $-sc$ range in a B-DNA duplex, is the one depicted in *Fig. 8* (top).

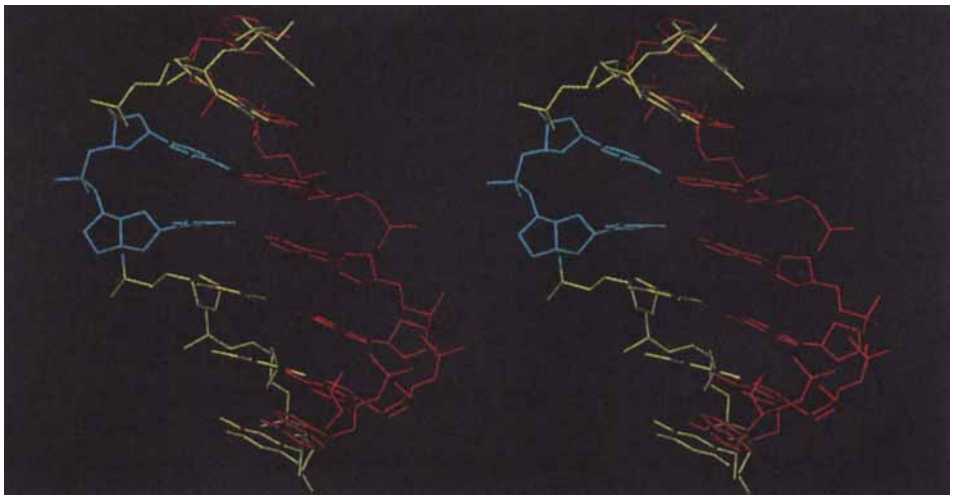

Fig. 7. *Stereoscopic view of the average of the last 10 ps of a 200-ps dynamics trajectory of the duplex d(A-A-A-A-A-A-A)·d(T-T-T-Y-T-T-T)* (Y = 5'-epi-bicyclodeoxythymidine). Solvent and H-atoms omitted, purine strand (red), pyrimidine strand (yellow), 5'-epi-bicyclodeoxythymidine modification (cyan).

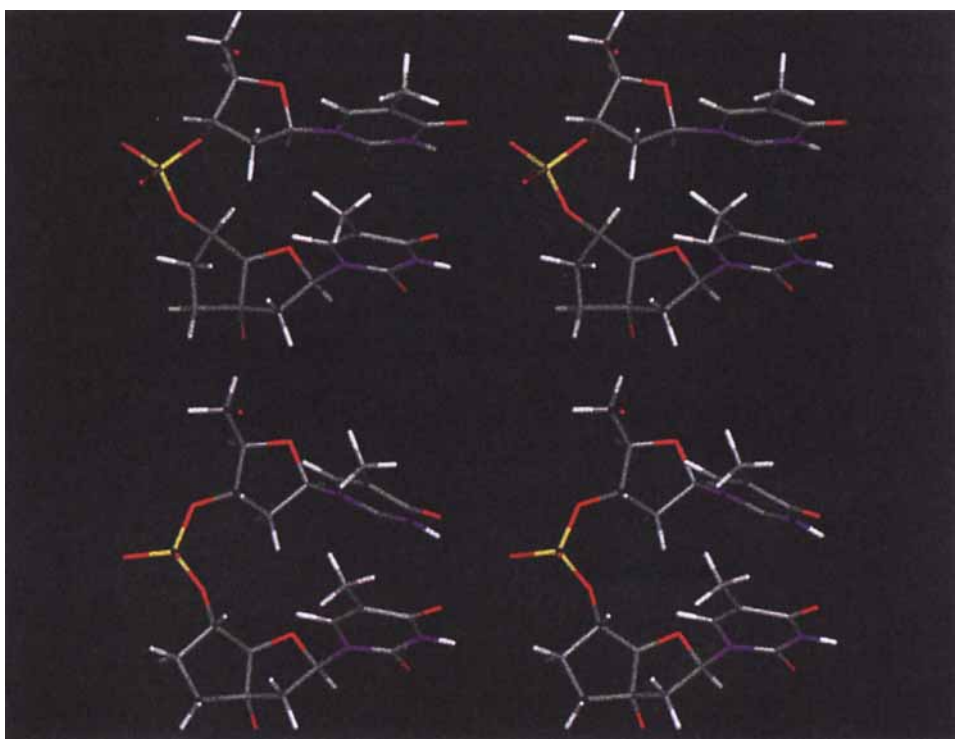

Fig. 8. *Stereoscopic views of the 5'-epi-bicyclothymidine residue with its 5'-situated neighbor taken from the dynamics simulation depicted in* Fig. 7. Top: initial conformation; bottom: average conformation of the last 10 ps of the 200-ps dynamics run.

This local conformation, however, has to be considered a strained conformation, since in its idealized version (all bonds ideally staggered) two nonbonded centers (C(5′) of the epi-bicyclonucleotide and C(2′) of the upstream-situated thymidine residue) would lie in bonding distance to each other. The close proximity of these two centers creates interresidue strain that is most effectively released within the restrictions of the imposed B-DNA structure by a change of conformation of the carbocyclic ring unit. This, however, at the expense of adopting an unfavorable 5′-epi-bicyclodeoxynucleoside conformation and nonideally arranged bases[12]).

8. Conclusions. – The 5′-epi-bicyclodeoxynucleosides can be considered as structural equivalents to the natural 2′-deoxynucleosides in which the C(5′)–O(5′) bond is preorganized in the *–sc* conformational range, thus deviating by *ca.* 180° from that observed in regular DNA duplexes. These nucleoside analogs, together with the parent bicyclonucleosides, can be used as sensors to probe the effect of local changes in torsion angle γ on duplex structure and stability. Oligonucleotides containing 5′-epi-bicyclodeoxynucleosides clearly show reduced pairing efficiency with respect to the natural reference sequences. With the aid of molecular modeling, this loss of pairing efficiency can be pinned down to an unfavorable conformational change imposed on the carbocyclic ring unit of the 5′-epi-bicyclodeoxynucleosides upon duplex formation. These experiments clearly show that the arrangement of torsion angle γ in the *–sc* range is not tolerated within the context of the *Watson-Crick* base-paired B-DNA. Furthermore, the absence of duplex formation of the fully modified **18** with $d(A_{10})$ also demonstrates that no other pairing mode, as *e.g.* the *Hoogsteen* or reversed-*Hoogsteen* mode, is accessible within the structural preorganization of the 5′-epi-bicyclodeoxynucleosides.

The results presented here, together with earlier findings in the bicyclonucleotide series, now provide a complete profile of the effect of torsion angle γ on structure and energetics of duplex formation. A change of this dihedral angle from the normally observed *+sc* orientation to the *anti*-periplanar (*ap*) arrangement is still compatible with *Watson-Crick* base-pair formation, however with lower pairing energy and only when C–G base pairs are involved in the duplex [20]. This orientation inherently prefers duplex formation according to the *Hoogsteen* or reversed-*Hoogsteen* mode (sequence composition permitting). The *–sc* orientation of this torsion angle, as is shown here, is no longer compatible with duplex formation according to the A- and B-type at all.

The studies in the oligo-bicyclodeoxynucleotide series thus complement the pioneering investigations of *Eschenmoser* and coworkers on homo-DNA, in which the effect of a change of torsion angle δ on DNA and RNA duplex structure was highlighted [21–23].

Financial support from the *Swiss National Science Foundation*, from *Ciba-Geigy AG*, Basel, and from the *Wanderstiftung*, Bern, is gratefully acknowledged.

[12]) We have measured the enthalpy of duplex formation in the case of the duplex **15**·$d(A_{10})$ from UV/melting curves at different duplex concentrations and have found it to be lower (less negative) by 2.5 kcal/mol compared to that of $d(T_{10})\cdot d(A_{10})$ under identical conditions. This energy closely corresponds to the difference for the two conformational forms of the epi-bicyclodeoxynucleosides (**7A** and **7B** in *Fig. 4*) thus showing that the destabilization is mainly enthalpic in nature and supporting the results from molecular modeling.

Experimental Part

General. Solvents for extraction: technical grade, distilled. Solvents for reactions: reagent grade, distilled over CaH_2 (MeCN, CH_2Cl_2, pyridine) or Na (THF). Reagents: if not otherwise stated, from *Fluka*, highest quality available. Enzymes: from *Boehringer Mannheim GmbH*; alkaline phosphatase, from calf intestine (1 mg/ml, EC 3.1.16.1); phosphodiesterase, from *Crotalus durissus* (2 mg/ml, EC 3.1.15.1). TLC: silica gel *G-25 UV$_{254}$* pre-coated glass plates, *Macherey-Nagel*; visualization by dipping in a soln. of anisaldehyde (10 ml), conc. sulfuric acid (10 ml), AcOH (2 ml), and EtOH (280 ml), followed by heating with a heat gun. Flash column chromatography (FC): silica gel; 30–60 μm, *J. T. Baker*. Medium-pressure liquid chromatography (MPLC): *Büchi* chromatography pump *668* attached to a *Knauer* chart recorder and *Büchi* UV/VIS filter photometer (254 nm); silica gel *60* (15–40 μm particle size, *Merck*); column 235 × 35 mm; flow 10 ml/min; t_R in min. HPLC: *Pharmacia-LKB-2249* gradient system attached to an *ABI-Kratos-Spectroflow-757* UV/VIS detector and a *Tarkan W + W* recorder *1100*. M.p.: not corrected. $[\alpha]_D$: *Perkin-Elmer-241* polarimeter, $d = 10$ cm, c in g/100 ml. Extinction coefficients ε of oligonucleotides determined according to [8]: $\varepsilon = 96\,000$ (**18**), 95 200 (**15**), 94 400 (**16**, **17**), 106 800 (**19**), and 106 600 (**20**, **21**). UV/Melting curves: *Varian-Cary-3E* UV/VIS spectrometer equipped with a temp.-controller unit and connected to a *Compaq-ProLinea-3/25-zs* personal computer; temp.-gradients of 0.5°/min, data points collected in intervals of *ca.* 0.3°; at temp. < 20°, the cell compartiment was flushed with N_2 to avoid condensation of H_2O on the UV cells; % hyperchromicity (wavelength) = $100[D(T)\text{-}D_0]/D_0$, with $D(T)$ = absorption at temp. T and D_0 = lowest absorption in the temp. interval; the transition temp. T_m was determined as described [24]. CD Spectra: *Jasco-J-500* spectropolarimeter connected to an *IBM-AT* personal computer; thermostating of the cell holder by a *Haake* circulating bath, temp. determination directly in the sample soln. IR: *Perkin-Elmer-1600-FTIR* spectrometer; in cm^{-1}. NMR: *Bruker-AC-300* spectrometer; δ in ppm rel. to $CHCl_3$ ($\delta(H)$ 7.25, δ(C) 77.00) or (D_6)DMSO (δ(H) 2.49, δ(C) 39.70); ^{13}C multiplicities from DEPT spectra; δ(P) in ppm rel. to 85% H_3PO_4 soln. (= 0 ppm; separated internal). MS: *Varian-MAT-CH-7A*; EI, ionisation energy 70 eV; FAB (positive), matrix solvent NOBA (= 3-nitrobenzyl alcohol); m/z (%). MALDI-TOF-MS: matrix DHAP (= 2,6-dihydroxyacetophenone) or THAP (= 2,3,5-trihydroxyacetophenone); m/z.

Mesylation and Separation of Anomers: General Procedure. To a stirred soln. of bicyclodeoxynucleosides **1** or **2** [6] in dry pyridine at 0° under Ar was added MsCl (1.4–1.5 equiv.). The mixture was allowed to warm to r.t. and stirring continued for 30–120 min. The reaction was quenched with $NaHCO_3$ soln. (300 ml) and the mixture extracted with AcOEt (2 × 200 ml). The combined org. phase was dried ($MgSO_4$) and evaporated and the residual pyridine coevaporated with toluene (2 × 10 ml). The resultant foam was purified, and anomers were separated by MPL chromatography.

(3′S,5′R)-1-[2′-Deoxy-5′-O-(methylsulfonyl)-3′,5′-ethano-α- and -β-D-ribofuranosyl]thymine (α/β-D-**3**). From α/β-D-**1** (1107 mg, 4.126 mmol; α-D/β-D 1:1.7), dry pyridine (80 ml), and MsCl (450 μl, 5.777 mmol). Purification and anomer separation (6% MeOH/CH_2Cl) gave α-D-**3** (526 mg, 37%) and β-D-**3** (797 mg, 56%), both as colorless foams.

Data of α-D-**3**: MPLC (6% MeOH/CH_2Cl_2): t_R 8.4. TLC (CH_2Cl_2/MeOH 9:1): R_f 0.55. IR ($CHCl_3$): 3525*m*, 3500–3200*m*, 2945*m*, 1710*s*, 1670*s*, 1485*s*. ^1H-NMR (300 MHz, (D_6)DMSO): 2.09–2.15, 2.21–2.39 (2*m*, 2 H–C(6′), 2 H–C(7′)); 2.17 (*s*, Me–C(5)); 2.57–2.64 (*m*, 2 H–C(2′)); 3.28 (*s*, $MeSO_3$); 4.51 (*d*, $J = 4.7$, H–C(4′)); 5.00 (*m*, H–C(5′)); 5.72 (br. *s*, OH); 6.30 (*dd*, $J = 2.0$, 5.6, H–C(1′)); 7.82 (*s*, H–C(6)); 11.41 (br. *s*, NH). ^{13}C-NMR: (75 MHz, $CDCl_3$): 11.57 (*q*, Me–C(5)); 28.44, 34.84 (2*t*, C(6′), C(7′)); 37.40 (*q*, $MeSO_3$); 45.48 (*t*, C(2′)); 79.68 (*d*, C(5′)); 84.24 (*d*, C(1′)); 86.51 (*s*, C(3′)); 87.89 (*d*, C(4′)); 109.49 (*s*, C(5)); 135.62 (*s*, C(6)); 149.88 (*s*, C(2)); 163.37 (*s*, C(4)). EI-MS: 345 (13, M^+), 221 (96), 177 (12), 153 (11), 125 (100), 110 (21), 107 (36).

Data of β-D-**3**: MPLC (6% MeOH/CH_2Cl_2): t_R 14.6. TLC (CH_2Cl_2/MeOH 9:1): R_f 0.50. IR ($CHCl_3$): 3525*m*, 3500–3200*m*, 2950*m*, 1710*s*, 1670*s*, 1485*s*. ^1H-NMR (300 MHz, (D_6)DMSO): 1.70–1.77, 2.10 2.36 (2*m*, 2 H–C(6′), 2 H–C(7′)); 1.90 (*s*, Me–C(5)); 2.35–2.37 (*m*, 2 H–C(2′)); 3.29 (*s*, $MeSO_3$); 4.15 (*d*, $J = 5.4$, H–C(4′)); 4.99 (*m*, H–C(5′)); 5.71 (br. *s*, OH); 6.34 (*dd*, $J = 5.1$, 10.0, H–C(1′)); 7.64 (*s*, H–C(6)); 11.40 (br. *s*, NH). ^{13}C-NMR: (75 MHz, (D_6)DMSO): 13.22 (*q*, Me–C(5)); 30.81, 36.06 (2*t*, C(6′), C(7′)); 38.84 (*q*, $MeSO_3$); 46.02 (*t*, C(2′)); 80.69 (*d*, C(5′)); 85.46 (*s*, C(3′)); 85.74 (*d*, C(1′)); 87.85 (*d*, C(4′)); 111.28 (*s*, C(5)); 136.58 (*d*, C(6)); 151.62 (*s*, C(2)); 164.85 (*s*, C(4)). EI-MS: 345 (8, M^+), 220 (50), 177 (4), 153 (5), 126 (100), 110 (8), 107 (17).

(3′S,5′R)-N^6-Benzoyl-9-[2′-deoxy-5′-O-(methylsulfonyl)-3′,5′-ethano-α- and -β-D-ribofuranosyl]adenine (α/β-D-**4**). From α/β-D-**2** (1340 mg, 3.513 mmol, α/β-D 2:1), dry pyridine (90 ml), and MsCl (408 μl, 5.270 mmol). Purification and anomeric separation (1% MeOH/CH_2Cl_2) gave α-D-**4** (940 mg, 58%) and β-D-**4** (546 mg, 34%), both as colorless foams.

Data of α-D-**4**: MPLC (1% MeOH/CH_2Cl_2): t_R 14.4. TLC (CH_2Cl_2/MeOH 9:1): R_f 0.46. IR ($CHCl_3$): 3600–3000*s*, 2940*m*, 1705*s*, 1605*s*, 1580*s*. ^1H-NMR (300 MHz, $CDCl_3$): 1.97–2.28 (*m*, 2 H–C(6′), 2 H–C(7′));

2.83–2.96 (*m*, 2 H–C(2′)); 3.02 (*s*, $MeSO_3$); 4.59 (*d*, J = 5.1, H–C(4′)); 4.94 (*ss*, J = 5.4, 7.6, H–C(5′)); 6.40 (*dd*, J = 2.2, 8.5, H–C(1′)); 7.31 (br. *s*, OH); 7.50 (*t*, J = 7.8, 2 arom. H); 7.60 (*d*, J = 7.4, 1 arom. H); 7.95 (*d*, J = 7.3, 2 arom. H); 8.12 (*s*, H–C(8)); 8.76 (*s*, H–C(2)); 9.26 (br. *s*, NH). ^{13}C-NMR (75 MHz, CDCl): 28.87, 35.97 (2*t*, C(6′), C(7′)); 38.50 (*q*, $MeSO_3$); 47.73 (*t*, C(2′)); 80.22 (*d*, C(5′)); 86.07 (*s*, C(3′)); 88.13 (*d*, C(4′)); 90.09 (*d*, C(1′)); 124.09 (*s*, C(5)); 127.90, 128.88 (2*d*, arom. C); 132.98, 133.29 (2*s*, arom, C); 143.83 (*d*, C(8)); 149.85 (*s*, C(6)); 150.32 (*s*, C(4)); 151.81 (*d*, C(2)); 164.60 (*s*, CO). EI-MS: 459 (2, M^+), 345 (4), 317 (4), 288 (8), 239 (97), 211 (100), 135 (24).

*Data of β-*D*-***4***:* MPLC (1% MeOH/CH_2Cl_2): t_R 17.8. TLC (CH_2Cl_2/MeOH 9:1): R_f 0.39. IR ($CHCl_3$): 3600–3000*s*, 2940*m*, 1710*s*, 1605*s*, 1580*s*. ^{1}H-NMR (300 MHz, $CDCl_3$): 1.79–1.88, 2.16–2.38 (2*m*, 2 H–C(6′), 2 H–C(7′)); 2.73 (*dd*, J = 9.4, 13.3, 1 H–C(2′)); 2.81 (*dd*, J = 5.6, 13.5, 1 H–C(2′)); 2.95 (*s*, $MeSO_3$); 4.45 (*d*, J = 5.4, H–C(4′)); 4.96 (*m*, H–C(5′)); 6.58 (*dd*, J = 5.6, 9.6, H–C(1′)); 7.01 (br. *s*, OH); 7.48–7.53, 7.56–7.66, 7.99–8.03 (3*m*, 5 arom. H); 8.34 (*s*, H–C(8)); 8.76 (*s*, H–C(2)); 9.26 (br. *s*, NH). ^{13}C-NMR (75 MHz, $CDCl_3$): 30.33, 35.42 (2*t*, C(6′), C(7′)); 38.54 (*q*, $MeSO_3$); 46.92 (*t*, C(2′)); 79.31 (*d*, C(5′)); 86.21 (*s*, C(3′)); 85.86 (*d*, C(4′)); 88.16 (*d*, C(1′)); 125.85 (*s*, C(5)); 128.04, 128.89 (2*d*, arom. C); 133.50, 133.63 (2*s*, arom. C); 141.46 (*d*, C(8)); 149.61 (*s*, C(6)); 151.69 (*s*, C(4)); 152.71 (*d*, C(2)); 165.15 (*s*, CO). EI-MS: 459 (1, M^+), 431 (2), 424 (3), 345 (4), 239 (8), 221 (30), 211 (100), 187 (81), 162 (65), 141 (32), 105 (44), 96 (58), 77 (31).

Acetyl Protection: General Procedure. To a stirred soln. of **3** or **4** in dry pyridine at 0° under Ar was added 4-(dimethylamino)pyridine (DMAP; 0.1 equiv.) followed by Ac_2O (1.2–3.0 equiv.). The mixture was allowed to warm to r.t. and stirring continued for 1–2 h. After cooling to 0°, the reaction was quenched with $NaHCO_3$ soln. (100 ml) and the mixture extracted with AcOEt (2 × 100 ml), dried ($MgSO_4$), and evaporated. The resultant material was purified by FC.

*(3′*S*,5′*R*)-1-[3′-*O*-Acetyl-2′-deoxy-5′-*O*-(methylsulfonyl)-3′,5′-ethano-β-*D*-ribofuranosyl]thymine* (**5**). From **3** (750 mg, 2.174 mmol), dry pyridine (35 ml), DMAP (26 mg, 0.217 mmol), and Ac_2O (246 µl, 2.609 mmol). FC (silica gel, CH_2Cl_2/MeOH 2:1) gave **5** (749 mg, 89%). Slightly yellow foam. IR ($CHCl_3$): 3530*m*, 2945*m*, 1705*s*, 1700*s*, 1485*s*. ^{1}H-NMR (300 MHz, $CDCl_3$): 1.90 (*s*, Me–C(5)); 2.03 (*s*, COMe); 2.06–2.11, 2.31–2.36 (2*m*, 2 H–C(6′), 2 H–C(7′), 1 H–C(2′)); 2.85 (*dd*, J = 5.1, 14.4, 1 H–C(2′)); 3.00 (*s*, $MeSO_3$); 4.59 (*d*, J = 5.1, H–C(4′)); 4.96–4.99 (*m*, H–C(5′)); 6.28 (*dd*, J = 5.1, 10.0, H–C(1′)); 7.33 (*s*, H–C(6)); 9.17 (br. *s*, NH). ^{13}C-NMR (75 MHz, $CDCl_3$): 12.45 (*q*, Me–C(5)); 21.60 (*q*, *C*O*Me*); 30.66, 32.92 (2*t*, C(6′), C(7′)); 38.43 (*q*, $MeSO_3$); 43.97 (*t*, C(2′)); 78.87 (*d*, C(5′)); 84.86 (*d*, C(1′)); 85.56 (*d*, C(3′)); 91.54 (*d*, C(4′)); 112.07 (*s*, C(5)); 134.46 (*d*, C(6)); 150.28 (*s*, C(2)); 163.54 (*s*, *C*OMe); 170.28 (*s*, C(4)). EI-MS: 388 (10, M^+), 286 (18), 203 (97), 125 (12), 107 (100), 81 (27).

*(3′*S*,5′*R*)-N^6-Acetyl-9-[3′-*O*-acetyl-2′-deoxy-5′-*O*-(methylsulfonyl)-3′,5′-ethano-β-*D*-ribofuranosyl]-N^6-benzoyladenine* (**6**). From **4** (520 mg, 1.132 mmol), dry pyridine (35 ml), DMAP (13 mg, 0.113 mmol), and Ac_2O (320 µl, 3.396 mmol). FC (silica gel, AcOEt/hexane 2:1) gave **6** (546 mg, 89%). Slightly brown foam. TLC (AcOEt/hexane 3:1): R_f 0.60. IR ($CHCl_3$): 3600–3100*m*, 2950*m*, 2860*m*, 1705*m*, 1700*m*, 1610*s*, 1580*m*. ^{1}H-NMR (300 MHz, $CHCl_3$): 1.99 (*s*, OCOMe); 2.24–2.31 (*m*, 2 H–C(6′), 2 H–C(7′)); 2.49 (*s*, NCOMe); 2.78–2.83, 2.93–2.98 (2*m*, 2 H–C(2′)); 2.87 (*s*, $MeSO_3$); 4.63 (*d*, J = 5.8, H–C(4′)); 4.93–4.95 (*m*, H–C(5′)); 6.40 (*dd*, J = 5.9, 8.8, H–C(1′)); 7.19 (*m*, 2 arom. H); 7.32 (*m*, 1 arom. H); 7.61 (*d*, J = 7.9, 2 arom. H); 8.31 (*s*, H–C(8)); 8.61 (*s*, H–C(2)). ^{13}C-NMR ($CDCl_3$, 75 MHz): 21.22 (*q*, OCO*Me*$_3$); 25.10 (*q*, NCO*Me*); 28.83, 32.99 (2*t*, C(6′), C(7′)); 38.10 (*q*, $MeSO_3$); 44.11 (*t*, C(2′)); 77.89 (*d*, C(5′)); 84.53 (*d*, C(4′)); 85.43 (*d*, C(1′)); 90.92 (*s*, C(3′)); 128.68 (*s*, C(5)); 128.28, 128.93 (2*d*, arom. C); 132.61, 133.86 (2*s*, arom C); 143.61 (*d*, C(8)); 150.61 (*s*, C(4)); 151.86 (*d*, C(2)); 152.64 (*s*, C(6)); 170.01, 171.66, 172.44 (3*s*, CO). EI-MS: 543 (1, M^+), 515 (5), 500 (5), 472 (2), 281 (6), 252 (10), 239 (20), 135 (18), 105 (100), 77 (66).

Inversion Reaction: General Procedure. A stirred suspension containing CsOAc (250 mmol) and **5** or **6** was heated (70–90°) in dry DMSO (25 ml) under Ar for 16 h to 5 d. After cooling to r.t., the suspension was diluted with $NaHCO_3$ soln. (50 ml) and extracted with AcOEt (2 × 60 ml). The combined org. phase was washed with H_2O (2 × 50 ml), dried ($MgSO_4$), evaporated, and purified by FC.

*(3′*S*,5′*S*)-1-(3′,5′-Di-*O*-acetyl-2′-deoxy-3′.5′-ethano-β-*D*-ribofuranosyl)thymine* (**7**). From **5** (700 mg, 1.809 mmol), CsOAc (4.80 g, 250 mmol), and dry DMSO (25 ml; 16 h at 90°). FC (silica gel, AcOEt/hexane 3:1) gave **7** (554 mg, 87%). White crystals. M.p. 115–117° $[\alpha]_D^{20} = -32.0$ (c = 0.5, MeOH). TLC (CH_2Cl_2/MeOH 9:1): R_f 0.31. IR ($CHCl_3$): 3530*m*, 1705*s*, 1700*s*, 1485*s*. ^{1}H-NMR (300 MHz, $CDCl_3$): 1.73–2.01 (*m*, 2 H–C(6′), 2 H–C(7′)); 1.86 (*d*, J = 1.0, Me–C(5)); 1.98 (*dd*, J = 9.5, 14.7, 1 H–C(2′)); 2.03, 2.04 (2*s*, COMe); 2.65–2.78 (*m*, 1 H–C(6′), 1 H–C(7′)); 2.85 (*dd*, J = 5.3, 14.7, 1 H–C(2′)); 4.34 (br. *s*, H–C(4′)); 5.01 (br. *s*, H–C(5′)); 6.12 (*dd*, J = 5.3, 9.5, H–C(1′)); 7.10 (*s*, H–C(6)); 10.08 (br. *s*, NH). ^{13}C-NMR (75 MHz, $CDCl_3$): 12.45 (*q*, *Me*–C(5)); 20.96, 21.52 (2*q*, CO*Me*); 30.02, 35.89 (2*t*, C(6′), C(7′)); 42.33 (*t*, C(2′)); 76.48 (*d*, C(5′)); 85.28 (*d*, C(1′)); 91.05 (*d*, C(4′)); 92.27 (*s*, C(3′)); 111.40 (*s*, C(5)); 134.85 (*d*, C(6)); 150.52 (*s*, C(2)); 164.0 (*s*, C(4)); 170.13, 170.18 (2*s*, *C*OMe). EI-MS: 352 (15, M^+), 292 (10), 232 (11), 227 (20), 167 (73), 125 (28), 107 (100), 79 (68), 43 (59).

(3′S,5′S)-N⁶-Benzoyl-9-(3′,5′-O-diacetyl-2′-deoxy-3′,5′-ethano-β-D-ribofuranosyl)adenine (**8**). From **6** (475 mg, 0.874 mmol), CsOAc (4.80 g, 250 mmol), and dry DMSO (25 ml; 5 d at 70°). FC (silica gel, 2% MeOH in AcOEt/hexane 3:1) gave **8** (336 mg, 83%). White foam. TLC (AcOEt/hexane 3:1): R_f 0.23. $[\alpha]_D^{20}$ = +63.8 (*c* = 0.5, MeOH). IR ($CHCl_3$): 3600–3100*m*, 2950*m*, 2860*m*, 1700*m*, 1610*s*, 1580*m*. ^{1}H-NMR (300 MHz, $CDCl_3$): 2.08, 2.13 (2*s*, OCOMe); 2.04–2.75 (*m*, 2 H–C(6′), 2 H–C(7′)); 2.46 (*dd*, *J* = 6.2, 14.8, 1 H–C(2′)); 3.01 (*dd*, *J* = 6.3, 14.9, 1 H–C(2′)); 4.54 (br. *s*, H–C(4′)); 5.07 (*d*, *J* = 3.6, H–C(5′)); 6.41 (*dd*, *J* = 6.3, 8.7, H–C(1′)); 7.48–7.53, 7.57–7.59, 8.00–8.04 (3*m*, 5 arom. H); 8.11 (*s*, H–C(8)); 8.76 (*s*, H–C(2)); 9.28 (br. *s*, NH). ^{13}C-NMR ($CDCl_3$, 75 MHz): 20.67, 21.22 (2*q*, *CO*Me); 29.01, 35.82 (2*t*, C(6′), C(7′)); 41.84 (*t*, C(2′)); 76.70 (*t*, C(5′)); 85.59 (*d*, C(4′)); 91.31 (*d*, C(1′)); 92.43 (*s*, C(3′)); 123.81 (*s*, C(5)); 127.77, 128.14 (2*d*, 4 arom. C); 132.19, 133.15 (2*s*, 2 arom. C); 141.67 (*d*, C(8)); 149.60 (*s*, C(6)); 151.32 (*s*, C(4)); 151.75 (*d*, C(2)); 165.04 (*s*, *C*OPh); 169.73, 169.98 (2*s*, *C*OMe). EI-MS: 465 (14, M^+), 437 (24), 403 (17), 361 (28), 210 (72), 178 (77), 135 (71), 107 (100), 77 (26).

Selective Saponification: General Procedure. A soln. of **7** or **8** in THF/MeOH/H_2O 5:4:1 was cooled to 0°. To this was added 0.2M NaOH. The mixture was kept at 0° (TLC monitoring). After completion, the mixture was neutralized with 0.2M HCl to pH 6.9 and evaporated. The residue was adsorbed on silica gel (500 mg, 2 × 10 ml MeOH) and evaporated again. FC gave the desired product in pure form.

(3′S,5′S)-1-(2′-Deoxy-3′,5′-ethano-β-D-ribofuranosyl)thymine (**9**). From **7** (500 mg, 1.420 mmol), THF/MeOH/H_2O 5:4:1 (25 ml), and NaOH (6 ml; 30 min). FC (CH_2Cl_2/MeOH 9:1) gave **9** (327 mg, 86%). White solid. TLC (AcOEt/hexane 3:1): R_f 0.08. IR (KBr): 3520*m*, 3500–3200*m*, 2940*m*, 2840*m*, 1670*s*, 1480*s*. H-NMR (300 MHz, (D_6)DMSO): 1.90 (*s*, Me–C(5)); 1.84–2.22, 2.50–2.57 (2*m*, 2 H–C(6′), 2 H–C(7′), 2 H–C(2′)); 3.89 (br. *s*, H–C(4′)); 4.25 (br. *s*, H–C(5′)); 5.04, 5.51 (2 br. *s*, OH); 6.22 (*dd*, *J* = 5.2, 10.1, H–C(1′)); 7.57 (*s*, H–C(5)). ^{13}C-NMR (75 MHz, (D_6)DMSO): 12.29 (*q*, Me–C(5)); 32.62, 37.47 (2*t*, C(6′), C(7′)); 44.49 (*t*, C(2′)); 75.70 (*d*, C(5′)); 80.55 (*d*, C(1′)); 88.70 (*s*, C(3′)); 97.51 (*d*, C(4′)); 110.11 (*s*, C(5)); 135.85 (*d*, C(6)); 150.78 (*s*, C(2)); 163.93 (*s*, C(4)). EI-MS: 268 (5, M^+), 143 (100), 127 (60), 99 (85), 81 (12).

(3′S,5′S)-N⁶-Benzoyl-9-(2′-deoxy-3′,5′-ethano-β-D-ribofuranosyl)adenine (**10**). From **8** (276 mg, 0.593 mmol), THF/MeOH/H_2O 5:4:1 (30 ml), and NaOH (1 ml; 75 min). FC (CH_2Cl_2/MeOH 9:1) gave **10** (191 mg, 85%). White solid. TLC (CH_2Cl_2/MeOH 9:1): R_f 0.25. IR (H_2O): 3600–3000*s*, 2950*m*, 1705*s*, 1610*s*, 1580*s*, 1510*s*. ^{1}H-NMR (300 MHz, (D_6)DMSO): 1.82–1.88, 2.02–2.18, 2.23–2.29 (3*m*, 2 H–C(6′), 2 H–C(7′)); 2.48–2.54, 2.94–3.02 (2*m*, 2 H–C(2′)); 4.05 (br. *s*, H–C(4′)); 4.05 (br. *s*, H–C(5′)); 5.00 (*d*, *J* = 3.2, OH–C(5′)); 5.62 (*s*, OH–C(3′)); 6.49 (*dd*, *J* = 5.1, 10.2, H–C(1′)); 7.65–7.70, 7.77–7.79 (2*m*, 5 arom. H); 7.77 (*m*, 1 arom. H); 8.16 (*d*, *J* = 7.1, 2 arom. H); 8.85 (*s*, H–C(8)); 8.88 (*s*, H–C(2)); 11.33 (*s*, NH). ^{13}C-NMR (75 MHz, (D_6)DMSO): 33.19, 37.67 (2*t*, C(6′), C(7′)); 45.45 (*t*, C(2′)); 75.79 (*d*, C(5′)); 85.07 (*d*, C(4′)); 87.25 (*s*, C(3′)); 97.48 (*d*, C(1′)); 126.97 (*s*, C(5)); 129.57, 129.69 (2*d*, arom. C); 133.55, 134.44 (2*s*, arom. C); 144.29 (*d*, C(8)); 151.48 (*s*, C(4)); 152.82 (*d*, C(2)); 153.30 (*s*, C(6)); 166.75 (*s*, CO). EI-MS: 381 (8, M^+), 266 (12), 242 (11), 241 (30), 240 (100), 136 (15).

Tritylation: General Procedure. To a soln. of **9** or **10** in dry pyridine containing activated 4 Å molecular sieves (100–200 mg), under Ar, was added $[(MeOH)_2Tr]CF_3SO_3$ (3.3–6 equiv.) [8] at r.t. or 40°. If necessary, further reagent was added gradually until all starting material had disappeared (TLC control). After 2–6.5 h, the reaction was quenched with $NaHCO_3$ soln. (50 ml), the mixture extracted with AcOEt (2 × 50 ml), dried ($MgSO_4$), and evaporated, and the residue purified by FC.

(3′S,5′S)-1-{2′-Deoxy-5′-O-[(4,4′-dimethoxytriphenyl)methyl]-3′,5′-ethano-β-D-ribofuranosyl}thymine (**11**). From **9** (315 mg, 1.175 mmol), dry pyridine (5 ml), 4 Å molecular sieves (100 mg), and $[(MeO)_2Tr]CF_3SO_3$ (1755 mg, 3.879 mmol; 2 h at r.t.). FC (silica gel, 1% Et_3N in hexane/AcOEt 1:3) gave **11** (503 mg, 64%). Pale yellow foam. TLC (AcOEt/hexane 3:1): R_f 0.44. IR (KBr): 3600–3200*m*, 3000*w*, 2950*w*, 2840*w*, 1700*m*, 1610*s*, 1580*s*, 1510*s*. ^{1}H-NMR (300 MHz, $CDCl_3$): 1.32–1.38 (*m*, 1 H, H–C(6′) or H–C(7′)); 1.60 (*dd*, *J* = 5.3, 13.7, 1 H, H–C(6′) or H–C(7′)); 1.75–1.98 (*m*, 2 H, H–C(6′) and/or H–C(7′)); 1.79 (*s*, Me–C(5)); 2.04–2.10 (*m*, 1 H–C(2′)); 2.40 (*dd*, *J* = 5.3, 13.7, 1 H–C(2′)); 2.68 (br. *s*, OH); 3.69 (br. *s*, H–C(4′)); 3.70, 3.71 (2*s*, *Me*O); 3.96 (*m*, H–C(5′)); 6.05 (*dd*, *J* = 5.2, 9.5, H–C(1′)); 6.75 (*d*, *J* = 8.9, 4 arom. H); 6.90 (*s*, H–C(6)); 7.14–7.24 (*m*, 5 arom. H); 7.30 (*d*, *J* = 8.6, 2 arom. H); 7.41 (*d*, *J* = 3.6, 2 arom. H); 8.87 (br. *s*, NH). ^{13}C-NMR (75 MHz, $CDCl_3$): 12.54 (*q*, *Me*–C(5)); 31.64, 37.88 (2*t*, C(6′), C(7′)); 46.25 (*t*, C(2′)); 55.13 (*q*, MeO); 77.69 (*d*, C(5′)); 84.53 (*d*, C(1′)); 86.01, 86.94 (2*s*, C(3′), Ar_2*C*Ph); 94.88 (*d*, C(4′)); 113.05, 113.12, 126.78, 127.77, 128.30, 130.16, 130.20 (7*d*, arom. C); 111.36 (*s*, C(5)); 134.49 (*d*, C(6)); 136.47, 136.65, 145.33 (3*s*, arom. C); 150.45 (*s*, C(2)); 158.49 (*s*, MeO); 163.74 (*s*, C(4)). EI-MS: 570 (2, M^+), 444 (4), 303 (100), 288 (60), 273 (38), 243 (31), 227 (48), 215 (23), 143 (45), 81 (27).

(3′S,5′S)-N⁶-Benzoyl-9-{2′-deoxy-5′-O-[(4,4′-dimethoxytriphenyl)methyl]-3′,5′-ethano-β-D-ribofuranosyl}-adenine (**12**). From **10** (147 mg, 0.385 mmol), dry pyridine (10 ml), 4 Å molecular sieves (200 mg), and $[(MeO)_2Tr]CF_3SO_3$ (in total 1047 mg, 2.313 mmol; 6.5 h at 40°). FC (silica gel, 1% Et_3N in CH_2Cl_2/MeOH 15:1) gave **12** (205 mg, 78%). White foam. TLC (AcOEt): R_f 0.62. ^{1}H-NMR (300 MHz, $CDCl_3$): 1.38–1.49, 1.51–1.55, 1.87–1.96, 1.99–2.07 (4*m*, 2 H–C(6′), 2 H–C(7′)); 2.45 (*dd*, *J* = 5.7, 13.5, 1 H–C(2′)); 2.63 (*dd*, *J* = 9.3, 13.5,

1 H–C(2')); 3.66, 3.67 (2*s*, MeO); 3.90 (br. *s*, H–C(4')); 4.03–4.07 (*m*, H–C(5')); 6.07 (*dd*, *J* = 5.7, 9.1, H–C(1')); 6.68 (*q*, *J* = 5.7, 4 arom. H); 7.09–7.40 (*m*, 7 arom. H); 7.42–7.51 (*m*, 5 arom. H); 7.90 (*s*, H–C(8)); 7.94 (*d*, *J* = 7.3, 2 arom. H); 8.62 (*s*, H–C(2)); 9.0 (vbr. *s*, OH); 9.34 (br. *s*, NH). ^{13}C-NMR ($CDCl_3$, 75 MHz): 31.19, 37.85 (2*t*, C(6'), C(7')); 45.15 (*t*, C(2')); 55.09, 55.16 (2*q*, MeO); 77.56 (*d*, C(5')); 85.62 (*d*, C(4')); 86.75, 86.94 (2*s*, C(3'), Ar_2CPh); 95.77 (*d*, C(1')); 123.28 (*s*, C(5)); 113.07, 126.82, 127.76, 127.93, 128.24, 128.75, 130.09, 130.16, 130.21, 132.73, 136.50, 145.36 (12*d*, arom. C); 141.65 (*d*, C(8)); 151.41 (*s*, C(4)); 152.43 (*d*, C(2)); 158.51 (*s*, C(6)); 163.50 (*s*, CO). FAB-MS (pos): 684 (1, $[M + 1]^+$), 604 (5), 461 (1), 353 (27), 303 (5), 240 (100), 192 (5).

Phosphoramidites: General Procedure. To a soln. of **11** or **12** in MeCN at 0° under Ar were added $(i\text{-}Pr)_2EtN$ (4 equiv.) and chloro(2-cyanoethoxy)(diisopropylamino)phosphine (2 equiv.). After 40–60 min, the reaction was quenched with $NaHCO_3$ soln. (5 ml), extracted with AcOEt containing 1% Et_3N (2 × 10 ml), dried ($MgSO_4$), evaporated, and purified by FC.

*(3'S,5'S)-1-{5'-O-[(2-Cyanoethoxy)(diisopropylamino)phosphino]-2'-deoxy-3'-O-[(4,4'-dimethoxytriphenyl)methyl]-3',5'-ethano-β-*D*-ribofuranosyl}thymine* (**13**). From **11** (480 mg, 0.842 mmol), MeCN (10 ml), $(i\text{-}Pr)_2EtN$ (581 µl, 3.368 mmol), and chloro(2-cyanoethoxy)(diisopropylamino)phosphine (376 µl, 1.684 mmol; 40 min). FC (silica gel, 1% Et_3N in hexane/AcOEt 1:1) gave **13** (505 mg, 78%). Pale yellow foam (1:1 mixture by ^{1}H- and ^{31}P-NMR). TLC (1% Et_3N in AcOEt/hexane 3:1): 0.61, 0.67. ^{1}H-NMR (300 MHz, $CDCl_3$): 1.12–1.18 (*m*, 2 Me_2CH); 1.21–1.32, 1.48–1.56 (2*m*, 2 H–C(6'), 2 H–C(7')); 1.79–1.86 (*m*, 1 H–C(2')); 1.84 (*s*, Me–C(5)); 2.26–2.30 (*m*, OCH_2CH_2CN); 2.51–2.62 (*m*, OCH_2CH_2CN); 2.76 (*dd*, *J* = 3.7, 13.8, 1 H–C(2')); 3.54–3.68 (*m*, 2 Me_2CH); 3.72 (*s*, MeO); 3.79 (br. *s*, H–C(4')); 3.89–3.95 (*m*, H–C(5')); 5.95–6.04 (*m*, H–C(1')); 6.89 (*s*, H–C(6)); 6.75 (*dd*, *J* = 3.0, 11.9, 2 arom. H); 7.14–7.23 (*m*, 5 arom. H); 7.28 (*d*, *J* = 8.8, 2 arom. H); 7.39 (*d*, *J* = 7.1, 2 arom. H); 7.91 (br. *s*, NH). ^{31}P-NMR (130 MHz, $CDCl_3$): 142.05, 142.23. EI-MS: 770 (1, M^+), 408 (6), 304 (100), 288 (11), 273 (49), 232 (53), 227 (62), 197 (25), 126 (67), 102 (52).

*(3'S,5'S)-N^6-Benzoyl-9-{3'-O-[(2-cyanoethoxy)(diisopropylamino)phosphino]-2'-deoxy-5'-O-[(4,4'-dimethoxytriphenyl)methyl]-3',5'-ethano-β-*D*-ribofuranosyl}adenine* (**14**). From **12** (198 mg, 0.290 mmol), THF (4 ml), $(i\text{-}Pr)_2EtN$ (202 µl, 1.160 mmol), and chloro(2-cyanoethoxy)(diisopropylamino)phosphine (130 µl, 0.580 mmol; 60 min). FC (silica gel, 1% Et_3N in hexane/AcOEt 3:1) gave **14** (166 mg, 65%). White foam (1:1 mixture by ^{1}H- and ^{31}P-NMR). TLC (1% Et_3N in AcOEt/hexane 3:1): 0.50, 0.57. ^{1}H-NMR (300 MHz, $CDCl_3$): 1.13–1.23 (*m*, 2 Me_2CH); 1.24–1.35, 1.89–2.01 (2*m*, 2 H–C(6'), 2 H–C(7')); 2.34–2.40 (*m*, OCH_2CH_2CN); 2.55–2.65 (*m*, OCH_2CH_2CN); 3.43–3.50 (*m*, 1 H–C(2')); 3.56–3.67 (*m*, 1 H–C(2')); 3.69, 3.71 (2*s*, MeO); 4.05 (br. *s*, H–C(4')); 4.31–4.33 (*m*, H–C(5')); 6.15–6.23 (*m*, H–C(1')); 6.66–6.73 (*m*, 4 arom. H); 7.10–7.19 (*m*, 4 arom. H); 7.25–7.54 (*m*, 7 arom. H); 7.95 (*s*, H–C(8)); 7.96 (*d*, *J* = 6.3, 1 arom. H); 7.94 (*d*, *J* = 7.3, 2 arom. H); 8.63 (*s*, H–C(2)); 8.94 (br. *s*, NH). ^{31}P-NMR ($CDCl_3$, 80 MHz): 141.68, 141.81. FAB-MS (pos): 884 (1, $[M + 1]^+$), 304 (20), 303 (100), 240 (16), 201 (5), 105 (16).

Synthesis of Oligodeoxynucleotides **15–21**. The synthesis of the oligonucleotides were performed on a *Pharmacia-Gene-Assembler-Plus*® connected to a *Compaq-ProLinea-3/25-zs* personal computer. All syntheses were carried out on the 1.3-µmol scale. Reagent soln. were prepared according to manufacturers protocol [25]. Phosphoramidite (0.1M) and 1*H*-tetrazole (0.5M) solns. were equal in conc. to those used for the synthesis of natural nucleotides. Detritylation times were extended to 60 s and coupling times to 14 min (only for those cycles containing the 5'-epi-bicyclonucleotides). Coupling efficiencies as monitored by on-line trityl assay were *ca.* 85%. The last step in all syntheses was the removal of the 5'-protected group (trityl-off mode). After synthesis, the solid support was suspended in conc. NH_3 soln. and left for 10–16 h at 55° to effect deprotection and cleavage. Evaporation, redissolution in H_2O, followed by filtration yielded the crude oligonucleotide soln. that was subsequently used for HPLC purification. All natural oligonucleotides that were used for comparison of biophysical properties were synthesized according to the standard procedure and purified by HPLC. Details for synthesis, HPLC purification, and anal. characterization by MALDI-TOF-MS are given in *Table 4*.

Enzymatic Degradation of Oligonucleotide **18**. A *ca.* 4 µM soln. of **18** (*ca.* 1 ml) in 10 mM *Tris*·HCl/0.15 mM NaCl (pH 7.0) was incubated at 37° with 2 µl of a soln. of phosphodiesterase from *Crotalus durissus* (2 mg/ml) and 5 µl of a soln. of alkaline phosphatase from calf intestine (1 mg/ml). The time course of hydrolysis was monitored by UV spectroscopy (260 nm).

Molecular Modeling of Duplex d(A-A-A-A-A-A-A)·d(T-T-T-Y-T-T-T) (Y = 5'-epi-bicyclodeoxythymidine). The duplex was built using canonical **B**-DNA torsion angles and *Watson-Crick* H-bonding patterns as implemented by *Biosym/Molecular Simulations' InsightII* biopolymer module. One C(3')–C(5') ethylene bridge was introduced to the central nucleotide of the pyrimidine strand, so that O(5') was pseudoaxially oriented, and torsion angles that corresponded with the 5'-epi-bicyclodeoxynucleoside **7A**. The purine strand, all unmodified nucleotides of the pyrimidine strand, and the modified sugar's nucleobase were then fixed, the torsion angles of the modified sugar were restrained, α (60°), β (−160°), γ (−86°), δ (116°), ε (160°), and ζ (−94°), while the newly constructed

Table 4. *HPLC Purification, MALDI-TOF-MS, and Yield of Oligonucleotides* **15–21**

Sequence	HPLC[a])	MALDI-TOF-MS		*OD* (260 nm) (yield [%])
		calc.	found	
15	DEAE: 20–60% *B* in 30 min; t_R 20 min	3006.1	3005.4	7.0 (6)
16	DEAE: 20–60% *B* in 30 min; t_R 16 min	3032.1	3031.9	6.8 (6)
17	DEAE: 20–60% *B* in 30 min; t_R 21 min	3032.1	3029.1	14.2 (12)
18	DEAE: 0–50% *B* in 20 min; t_R 22 min	3530.5	3532.0	16.8 (13)
19	DEAE: 30–80% *B* in 30 min; t_R 18 min	3097.2	3101.4	6.3 (5)
20	DEAE: 15–80% *B* in 30 min; t_R 29 min	3124.1	3125.0	8.2 (6)
21	DEAE: 15–75% *B* in 30 min; t_R 28 min	3124.1	3125.0	7.4 (5)

[a]) *Nucleogen DEAE 60-7*, 125 × 4.0 mm (*Macherey & Nagel*); *A*: 20 mM KH_2PO_4 in H_2O/MeCN 4:1, pH 6.0; *B*: *A* + 1M KCl; flow 1 ml/min; detection 260 nm.

bicyclic sugar system was relaxed *in vacuo* by *Polak-Ribiere* conjugate gradient (PRCG) minimization to a gradient < 0.1 kJ/Åmol. All the calculations were carried out as implemented by the esff forcefield of *Biosym/Molecular Simulations' Discover 95.0* package, on an *SGI Indigo 2* workstation. All restraints were then removed and a 5-Å sphere of H_2O molecules (388) was placed around the duplex; 12 random H_2O molecules were replaced with Na^+ to obtain overall charge neutrality. The nonbonded coulombic electrostatic cutoff was extended to 20.0 Å, and a distance-dependent dielectric constant of 1.0 was used. The unrestrained, solvated duplex was then subjected to PRCG minimization to a gradient of < 0.05 kJ/Åmol, followed by 200 ps of dynamics at 298.0 K (1.5 fs time step). The velocities were recorded every 1.0 ps throughout the simulation.

REFERENCES

[1] M. Bolli, P. Lubini, C. Leumann, *Helv. Chim. Acta* **1995,** *78,* 2077.
[2] J.C. Litten, C. Epple, C. Leumann, *Bioorg. Med. Chem. Lett.* **1995,** *5,* 1231.
[3] A. De Mesmaeker, R. Häner, P. Martin, H.E. Moser, *Acc. Chem. Res.* **1995,** *28,* 366.
[4] J.F. Milligan, M.D. Matteucci, J.C. Martin, *J. Med. Chem.* **1993,** *36,* 1923.
[5] N.T. Thuong, C. Hélène, *Angew. Chem.* **1993,** *105,* 697.
[6] M. Tarköy, M. Bolli, B. Schweizer, C. Leumann, *Helv. Chim. Acta* **1993,** *76,* 481.
[7] M. Tarköy, C. Leumann, *Angew. Chem.* **1993,** *105,* 1516.
[8] M. Tarköy, M. Bolli, C. Leumann, *Helv. Chim. Acta* **1994,** *77,* 716.
[9] M. Bolli, C. Litten, R. Schütz, C. Leumann, *Chemistry Biology* **1996,** *3,* 197.
[10] W. Saenger, 'Principles of Nucleic Acid Structure'. Springer-Verlag, New York, 1984.
[11] O. Mitsunobu, *Synthesis* **1981,** 1.
[12] IUPAC-IUB, Abbreviations and Symbols for Nucleic Acids, Polynucleotides, and their Constituents, *Pure Appl. Chem.* **1983,** *55,* 1273.
[13] F. Mohamadi, N.G.J. Richards, W.C. Guida, R. Liskamp, M. Lipton, C. Caufield, G. Chang, T. Hendrickson, W.C. Still, *J. Comput. Chem.* **1990,** *11,* 440.
[14] D.B. Davies, *Prog. NMR Spectrosc.* **1978,** *12,* 135.
[15] H. Rosemeyer, G. Toth, B. Golankiewicz, Z. Kazimierczuk, W. Bourgeois, U. Kretschmer, H.-P. Muth, F. Seela, *J. Org. Chem.* **1990,** *55,* 5784.
[16] W.C. Still, A. Tempczyk, R.C. Hawley, T. Hendrickson, *J. Am. Chem. Soc.* **1990,** *112,* 6127.
[17] U. Pieles, W. Zürcher, M. Schär, H.E. Moser, *Nucleic Acids Res.* **1993,** *21,* 3191.
[18] D.S. Pilch, C. Levenson, R.H. Shafer, *Proc. Natl. Acad. Sci. U.S.A.* **1990,** *87,* 1942.
[19] M. Egli, L.D. Williams, C.A. Frederick, A. Rich, *Biochemistry* **1991,** *30,* 1364.
[20] J. Hunziker, C. Leumann, in 'Modern Synthetic Methods', Eds. B. Ernst and C. Leumann, Verlag Helvetica Chimica Acta, Basel, 1995, Chapt. 5, pp. 331–417.
[21] A. Eschenmoser, M. Dobler, *Helv. Chim. Acta* **1992,** *75,* 218.
[22] M. Böhringer, H.-J. Roth, J. Hunziker, M. Göbel, R. Krishnan, A. Giger, B. Schweizer, J. Schreiber, C. Leumann, A. Eschenmoser, *Helv. Chim. Acta* **1992,** *75,* 1416.
[23] J. Hunziker, H.-J. Roth, M. Böhringer, A. Giger, U. Diederichsen, M. Göbel, R. Krishnan, B. Jaun, C. Leumann, A. Eschenmoser, *Helv. Chim. Acta* **1993,** *76,* 259.
[24] L.A. Marky, K.J. Breslauer, *Biopolymers* **1987,** *26,* 1601.
[25] 'Gene Assembler® Special, Users Manual, Vers. 1.51', Pharmacia LKB Biotechnology AB, Uppsala, Sweden.